Journal of Medicinal Chemistry

Article

pubs.acs.org/jmc

Influence of Chlorine or Fluorine Substitution on the Estrogenic Properties of 1-Alkyl-2,3,5-tris(4-hydroxyphenyl)-1*H*-pyrroles

Anja Schäfer,[†] Anja Wellner,[†] Martin Strauss,[†] Andreas Schäfer,[‡] Gerhard Wolber,[†] and Ronald Gust*[,†,§]

[†]Institute of Pharmacy, Freie Universität Berlin, Königin-Luise-Strasse 2+4, D-14195 Berlin, Germany

[‡]Institute of Chemistry and Biochemistry, Freie Universität Berlin, Takustrasse 3, D-14195 Berlin, Germany

[§]Department of Pharmaceutical Chemistry, Institute of Pharmacy, Center for Molecular Biosciences Innsbruck, CCB—Centrum for Chemistry and Biomedicine, University of Innsbruck, Innrain 80/82, A-6020 Innsbruck, Austria

Supporting Information

ABSTRACT: In continuation of our previous work, several 1-alkyl-2,3,5-tris(4-hydroxyphenyl)aryl-1*H*-pyrroles with chlorine or fluorine substituents in the aryl residues were synthesized and tested for estrogen receptor (ER) binding at isolated ERα/ERβ receptors (HAP assay) and in transactivation assays using ERα-positive MCF-7/2a as well as U2-OS/ERα and U2-OS/ERβ cells. In the competition experiment at ERα the compounds displayed very high relative binding affinities of up to 37% (determined for **8m**) but with restricted subtype selectivity (e.g., ERα/ERβ (**8m**) = 9). The highest estrogenic potency in ERα-positive MCF-7/2a cells was determined for 2,3,5-tris(2-fluoro-4-hydroxyphenyl)-1-propyl-1*H*-pyrrole **8m** (EC_{50} = 23 nM), while in U2-OS/ERα cells 2-(2-fluoro-4-hydroxyphenyl)-3,5-bis(4-hydroxyphenyl)-1-propyl-1*H*-pyrrole **8b** (EC_{50} = 0.12 nM) was the most potent agonist, only 30-fold less active than estradiol (E2, EC_{50} = 0.004 nM). In U2-OS/ERβ cells for all pyrroles no transactivation could be observed, which indicates that they are selective ERα agonists in cellular systems.

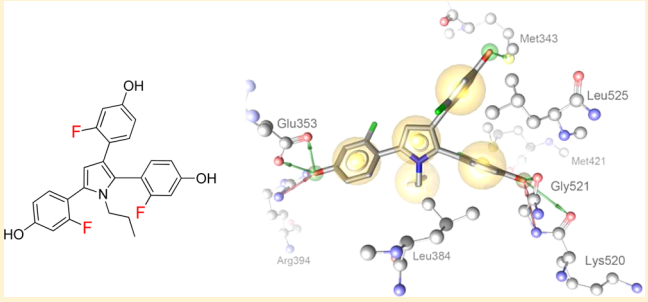

INTRODUCTION

As estrogen receptors (ERα and ERβ) play an important role in the growth of hormone-dependent breast cancer, selective estrogen receptor modulators (SERMs) such as tamoxifen (TAM, active metabolite 4-OHT; see Figure 1) or raloxifene (RAL), which act at the breast as anti-estrogens, are suitable drugs for the treatment of this disease. Unfortunately, only a very limited number of related SERMs are available for therapeutical use, and new drugs (e.g., lasofoxifene and bazedoxifene[1−3]), apart from only being approved for the treatment of osteoporosis, possess merely minor differences in their activities and effects compared to TAM or RAL.

Immunohistochemical analyses suggest that ERβ may have a dominant role in the healthy mammary gland, and its expression significantly decreases in cancer and metastatic lymph node tissues.[4−7] ERβ appears to suppress the function of ERα through different mechanisms. Overexpression of ERα is frequently observed in the early stage of breast cancer[8] and is accompanied by increased cell proliferation and tumor growth.[9]

This finding opens up the possibility of designing drugs that distinguish between malignant and nonmalignant breast tissue. If an ERα selective compound could be further equipped with an antagonistic hormonal profile, it could be an effective drug for the treatment of the mammary carcinoma. Therefore, as a first step we created molecules that bind exclusively to ERα to obtain a deeper insight into the requirements for ERα selectivity and estrogenic action.

Using propylpyrazole triol (PPT; for structural formulas see Figure 1) as lead structure,[10,11] we developed triarylpyrroles[12−14] as selective ERα agonists. Selected compounds are depicted in Figure 1. Unfortunately, type A pyrroles showed high susceptibility to oxidation reactions with only limited half-life for pharmacological studies (see below).[12] In contrast, the type B pyrroles displayed sufficient stability to study ER interaction.[13] These compounds demonstrated high selectivity for ERα depending on alkyl chains at the heterocyclic core.

In this part of our structure−activity study, we try to optimize the hormonal effects by introduction of chlorine or fluorine substituents in the aromatic rings. All compounds were evaluated for ER binding in a competition experiment with radiolabeled estradiol ([^{3}H]E2) as well as in transactivation experiments.

SYNTHESIS

The 2,3,5-triarylpyrroles were obtained following a synthetic route described earlier.[13,15]

As it was not commercially available, precursor **3a** had to be synthesized by reacting chloroform with 2-fluoro-4-methoxybenzaldehyde in DMF under basic conditions to form the α-trichloromethylcarbinol **1** (Scheme 1).[16]

Received: June 19, 2012
Published: October 8, 2012

dx.doi.org/10.1021/jm300860j | J. Med. Chem. 2012, 55, 9607−9618

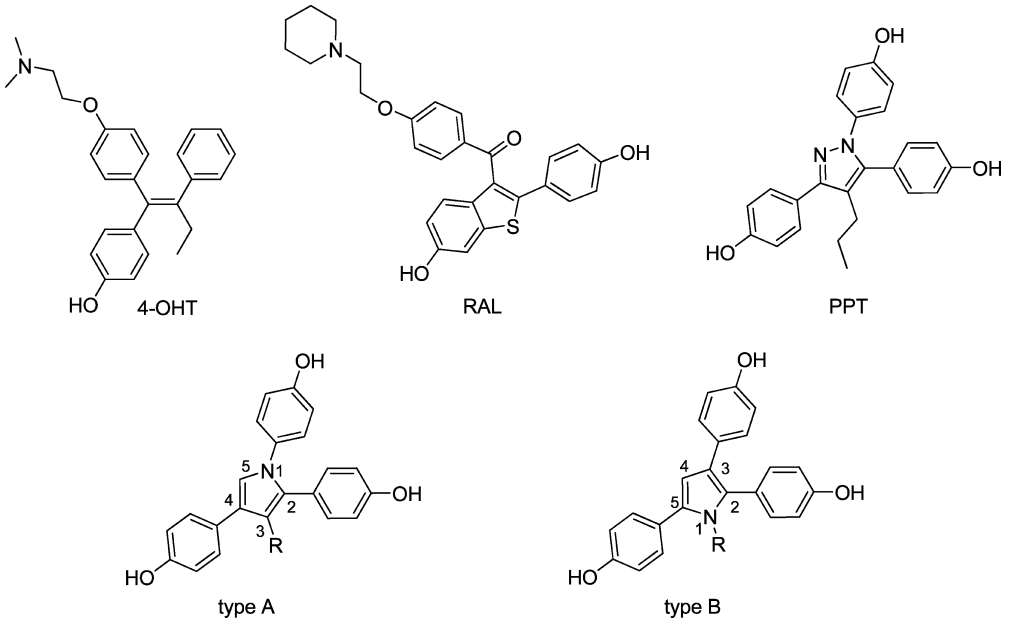

Figure 1. Ligands of the ER: 4-hydroxytamoxifen (4-OHT), raloxifene (RAL), propylpyrazole triol (PPT),[11] and type A (1,2,4-triaryl-3-alkylpyrroles) and type B (2,3,5-triaryl-1-alkylpyrroles) pyrroles.[12,13]

Scheme 1. Synthesis of Precursor 3a[a]

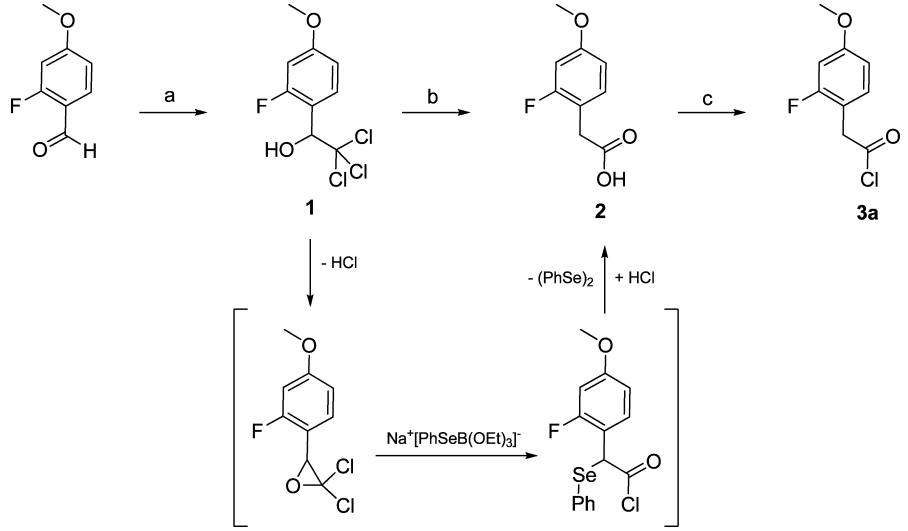

[a]Conditions: (a) −9 °C, dry DMF, KOH, dry methanol, 3 h, toluene, 1 N HCl; (b) dry ethanol, diphenyldiselenide, $NaBH_4$, NaOH, 40 °C, 36 h, 1 N HCl; (c) $SOCl_2$, reflux gently, 1 h.

In the subsequent reaction, the phenylseleno(triethyl)borate complex was generated from diphenyl diselenide and $NaBH_4$ in ethanol. The phenylseleno moiety then acts as a nucleophile at the dichloroepoxide prevalent in basic solution to form the α-phenylselenylacetyl chloride as an intermediate. The isolation of diphenyldiselenide after acidification points to the participation of an additional equivalent of $PhSeB(OEt)_3^-$ on the elimination of phenylselenide, yielding the phenylacetic acid **2**.[17] In the final step **2** was converted to the acid chloride **3a** by warming in thionyl chloride.

In a Friedel−Crafts acylation the acid chlorides **3a**,**b** and the respective anisoles (Scheme 2, method d) gave the desoxybenzoines **4a**−**e** which were then reacted with α-bromoketones **5a**,**b**,**d** to obtain the 1,2,4-tris(4-methoxyphenyl)butane-1,4-diones **6a**−**c**,**e**−**h** (Scheme 2, method e). Condensation of the latter with the appropriate primary amine (→**7a**−**m**; see Scheme 2, method f) and ether cleavage with BBr_3 (Scheme 2, method g) yielded the pyrroles **8a**−**m**.

RESULTS

Stability. The stability of the new compounds in aqueous solution was studied exemplarily on **8b**, **8h**, and **8m** by HPLC analysis (RP18 column, mobile phase of methanol/H_2O = 7/3, detection 265 nm). Stock solutions of compounds in methanol were diluted with PBS (pH 7.3) to a final concentration of 10^{-5} M and kept at 37 °C (for details see Experimental Section). As expected from our earlier studies,[12,13] the −I effect of substituents on the phenol rings at C2 and C5 and an alkyl chain at N1 increased the stability. During 195 h, **8b** ($t_{1/2}$ = 745 h), **8h** ($t_{1/2}$ = 1474 h), and **8m** ($t_{1/2}$ = 1055 h) degraded only

dx.doi.org/10.1021/jm300860j | J. Med. Chem. 2012, 55, 9607−9618

Scheme 2. Synthesis of Fluorine- or Chlorine-Substituted Type B 2,3,5-Triarylpyrroles[a]

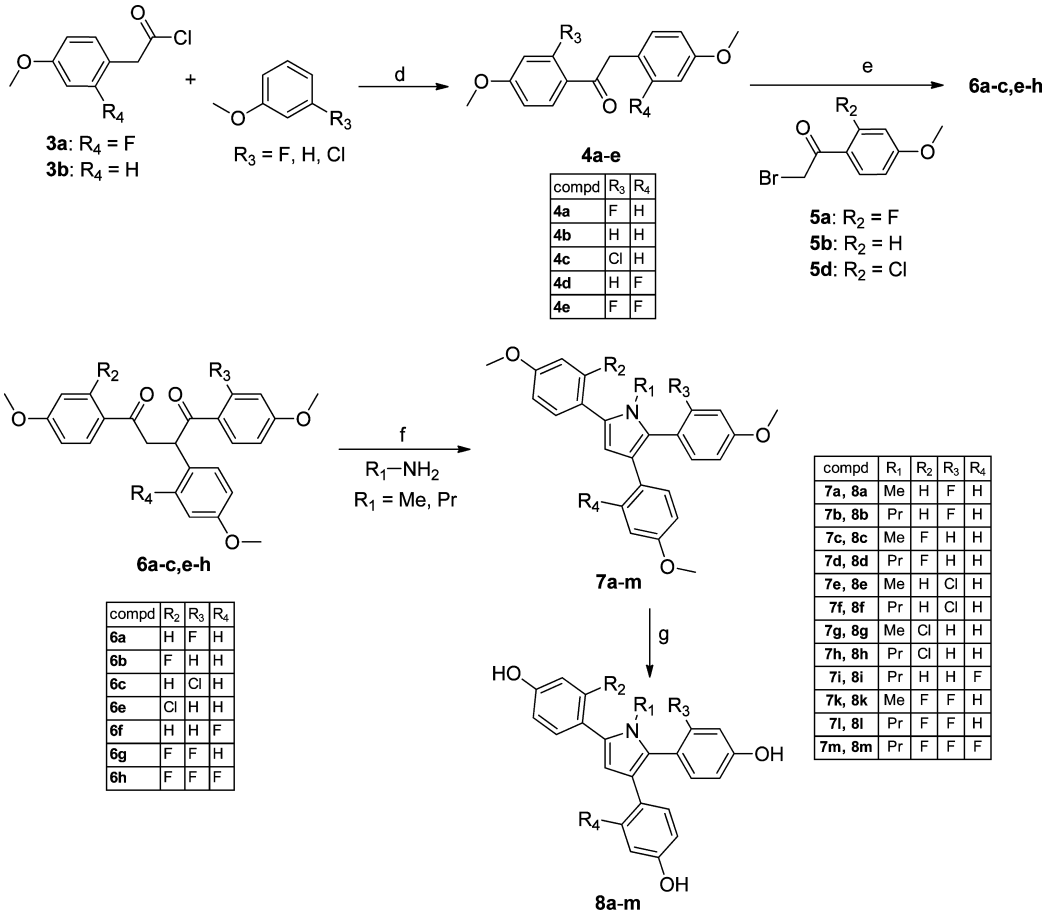

[a]Conditions: (d) dry DCM, 0 °C, $AlCl_3$; (e) dry THF, −78 °C, KHMDS solution; (f) dry ethanol, *p*-toluenesulfonic acid, reflux, appropriate amine, 3 h; (g) dry DCM, BBr_3, 0 °C.

marginally (see Figure 2). This is a clear improvement compared to compounds **5c** ($t_{1/2}$ = 256 h)[13] and **6d** ($t_{1/2}$ = 169 h)[12] (for formulas see Table 1).

Rotational Isomers. Halides (F or Cl) in ortho-position on the aromatic rings hinder the free rotation around the sp^2–sp^2 axis, resulting in a distereomeric splitting of the N–CH_2 protons in the NMR spectra of **8b**, **8f**, **8l**, and **8m**.

The signals of the N–CH_2 protons in the ^{1}H NMR of **8b** measured at room temperature are depicted in Figure 3 (J = 7.3 Hz, $\Delta\nu$ = 28 Hz). Heating the NMR solution to 409 K fused the signals to the expected triplet. From the coalescence temperature T_c = 353 ± 5 K the rotational barrier of the aromatic ring was calculated using the Eyring equation.[18] The Gibbs free energy for rotation of $\Delta G^{\ddagger}_c$ = 17.74 ± 0.25 kcal/mol was below the 25 kcal/mol necessary for separation of rotational isomers at room temperature.[19] The data obtained indicate that **8b** would have to be cooled to approximately −40 °C to obtain atropisomers which would have a half-life of 6 h, allowing a chromatographic separation and subsequent NMR characterization.

In order to investigate if the rotational isomers are of relevance for in vitro studies, the measurements were performed at 310 K (see Figure S1 in Supporting Information). Under these conditions the rotational isomers exchange within 0.2 s, so their existence is of no importance for cell culture experiments.

Relative Binding Affinity (RBA). All compounds were tested in a competition experiment (hydroxylapatite (HAP) assay) using radiolabeled estradiol ([^{3}H]E2) and hERα or hERβ (for details see Experimental Section). 2,3,5-Tris(4-hydroxyphenyl)-1-propyl-1*H*-pyrrole **5c**[13] and 1,2,4-tris(4-hydroxyphenyl)-3-propyl-1*H*-pyrrole **6d**[12] displaced E2 from the LBD of ERα with RBAs of 4.9% and 1.85%, respectively. At ERβ no

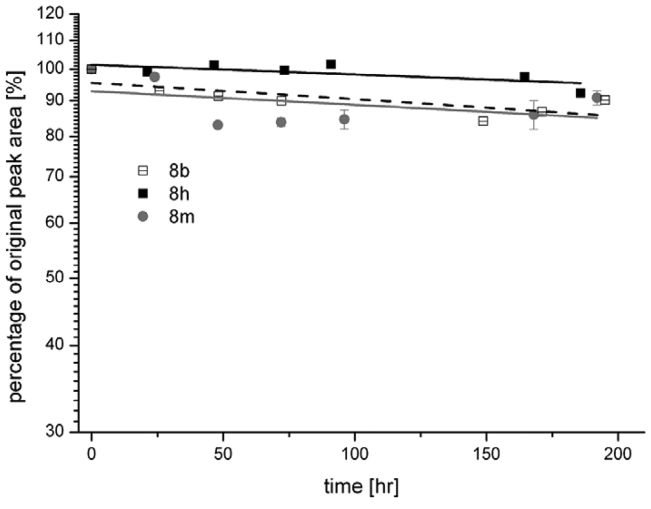

Figure 2. Percentage of original peak area over time diagram for compounds **8b**, **8h**, and **8m** (for HPLC method see Experimental Section). Values reflect ±SD of three determinations.

dx.doi.org/10.1021/jm300860j | J. Med. Chem. 2012, 55, 9607−9618

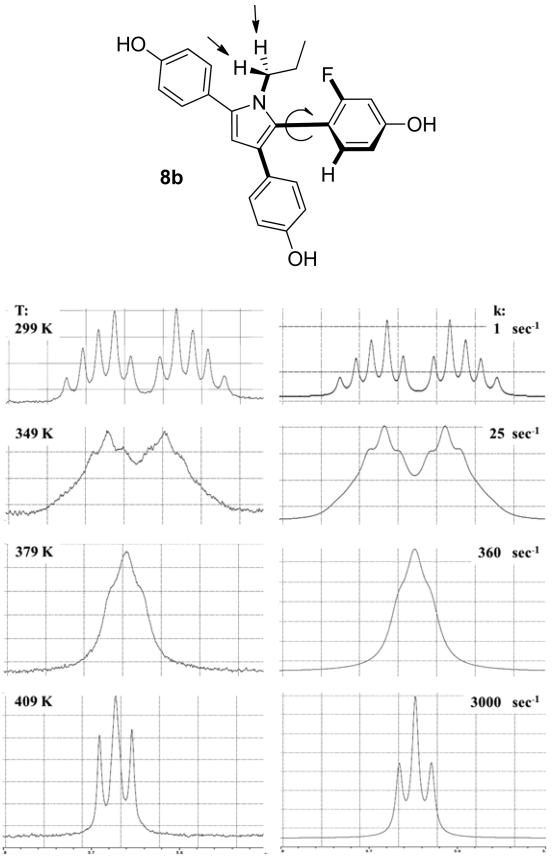

Figure 3. Temperature dependent ^{1}H NMR spectra (400 MHz) of **8b** in DMSO-d_6: partial NMR spectra at 299, 349, 379, and 409 K: (left) observed spectra of the protons in the N-CH_2- group (see arrows in formula); (right) computer line shape simulation obtained with the rate constants (k) indicated.

measurable RBA could be observed (Table 1). An additional N-atom at position 5 of **6d**, resulting in the reference compound PPT, increased the binding affinity to ERα (10.1%) and ERβ (0.5%) with an ERα/β ratio of 20.2.

Halogen substitution in the aromatic rings of the type B pyrroles increased the affinity not only to ERα but also to ERβ. **8m** and **8i** displayed the highest RBA to ERα (37% and 36%, respectively) with an α/β-ratio of 9 and 4.7.

From the data listed in Table 1, the structural requirements for high ER binding can be deduced. All pyrroles bearing a propyl chain bind better to ERα and ERβ than their respective methyl chain bearing congeners, indicating stronger hydrophobic contacts of the alkyl chain in the LBD.

Substitution of the aromatic rings with chlorine or fluorine increased the RBA values at both ER. In the *N*-methyl series F and Cl containing congeners bind with comparable affinity, while their *N*-propyl derivatives showed a higher affinity to ERα if they are F-substituted. At ERβ the F and Cl substitution caused comparable effects (compare **8b** and **8f**). Therefore, we refrained from the synthesis of further Cl-containing type B pyrroles.

The position but not the number of F substituents in the 2,3,5-tris(4-hydroxyphenyl)-1-propyl-1*H*-pyrrole is of high importance for the binding to ERα. The RBAs at ERβ remain, with exception of **8i** (RBA= 7.6%), nearly unchanged at about RBA $\approx$ 4.

The RBA values of the monofluorinated compounds increased in the series R_2 = F (**8d**, 13.0%) < R_3 = F (**8b**, 22.6%) < R_4 = F (**8i**, 36%). An additional F substituent can only increase the RBA of **8d** but not that of **8b**. The pyrrole **8l** (23.3%) showed nearly the same affinity as **8b**. Furthermore, the RBA of 37% calculated for **8m** demonstrates that the fluorine at R_4 is of highest significance for the binding to ERα (see Figure 4).

Estrogenic Activity in MCF-7 Cells. In order to evaluate the consequence of ER binding, transcription activation in ERα-positive MCF-7 cells stably transfected with the reporter plasmid ERE_{wtc}luc (MCF-7/2a cells)[20,21] (Figure 5 and Table 2) was evaluated[22] and compared with those of the endogenous ligand E2.

In MCF-7/2a cells, the pyrroles **8b**, **8f**, **8l**, **8m** and also PPT reached an intrinsic activity (IA) of 100% at 1 μM, while **8i** and **8k** were partial agonists with IAs of 50% and 78%, respectively. Compounds **8a**, **8c**, **8d**, and **8e** showed IAs between 40% and 70%. Their curves are characterized by a decrease of IA at higher concentrations. Such effects were also observed for **8b**, **8f**, and **8l**. **8g** and **8h** were completely inactive. Because partial agonists may have an antagonistic profile, the compounds were tested for antagonistic activity. However, none of them could antagonize the effect of 10^{-9} M E2 (data not shown).

The calculated EC_{50} values indicated that higher effects were achieved with compounds bearing a propyl chain at the nitrogen. Halides in the C2-standing phenolic ring of the propyl derivative **5c** (→**8b**, **8f**) did not change the hormonal potency (EC_{50} = 50−70 nM), while 2-F substituents in the C3- or C5-aryl ring (**8i**, **8l**, and **8m**) increased the hormonal potency to EC_{50} = 23−30 nM. These data obtained with the ERα-positive MCF-7/2a cell line correlated well with the RBA values determined in the HAP assay using hERα.

A further indication of hormonal activity is the regulation of the ER level in MCF-7 cells. With the exception of **8i**, which is a partial agonist (see Figure 5), the compounds with profiles of full agonists and the highest RBA values caused a clear down-regulation of the estrogen receptor (10 μM; see Figure S2). Their influence decreased in the series **8m** > **8l** > **8f** > **8b**. These compounds were more active than PPT at 10 μM and E2 at 1 μM. A depletion of ERα comparable to those of the reference substances E2 and PPT was detected for **8d**, **8e**, **8h**, **8i**, and **8k**, while **8a**, **8c**, and **8g** had no influence on the ERα level.

In order to verify the binding of the triarylpyrroles in the ligand binding domain (LBD) of ERα, compounds **6d**, **5c**, and **8l** (1 μM), respectively, were co-incubated with 4-OHT (0.1 μM) in MCF-7/2a cells. As outlined in Figure 6, 4-OHT severely decreased the capacity of **6d**, **5c**, and **8l** to induce luciferase expression, ascertaining that ERα was involved in the transactivation process. In addition, the compounds were added to the cells 1 and 3 h before addition of 4-OHT. If the pyrroles were added to the cells 1 or 3 h before 4-OHT, a slight tendency of increasing activity could be observed.

Transactivation in U2-OS Cells. To demonstrate ER-subtype selective transactivation, all compounds were tested in U2-OS/α and U2-OS/β cells transiently transfected with the plasmid pSG5-ERα or pSG5-ERβ FL (Table 2) and the reporter plasmid p$(ERE)_2$-luc$^+$.

With U2-OS/α cells a clear concentration−activity relation is given (no decrease of activation at 10 μM), so IAs and EC_{50} values could be exactly evaluated: **8a**, **8c**, **8d**, **8e**, **8f**, **8k**, and **8l** were full agonists; the other compounds were partial agonists with an IA between 46% and 79% (1 μM). Interestingly, **8g** and

dx.doi.org/10.1021/jm300860j | J. Med. Chem. 2012, 55, 9607−9618

Table 1. Binding Affinity for ERα and ERβ of 8a−m, 5c, 6d, PPT, and E2[a]

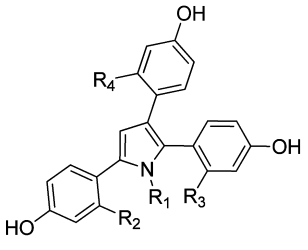

5c, 8a-m

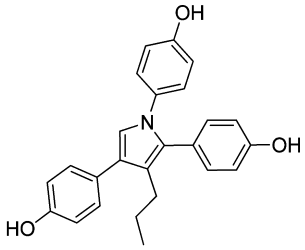

6d

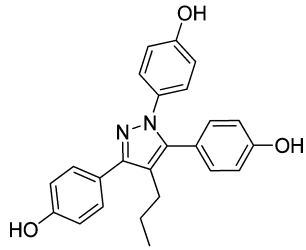

PPT

					HAP assay: rel binding affinity (%)		
compd	R_1	R_2	R_3	R_4	ERα	ERβ	ERα/ERβ
5c[b]	Pr	H	H	H	4.9	<0.01	>490
8a	Me	H	F	H	2.0	<0.3	>6.7
8b	Pr	H	F	H	22.6	3.7	6.1
8c	Me	F	H	H	3.2	1.8	1.8
8d	Pr	F	H	H	13.0	4.5	2.9
8e	Me	H	Cl	H	3.9	1.2	3.3
8f	Pr	H	Cl	H	11.5	3.1	3.7
8g	Me	Cl	H	H	3.9	1.7	2.3
8h	Pr	Cl	H	H	9.0	2.4	3.8
8i	Pr	H	H	F	36.0	7.6	4.7
8k	Me	F	F	H	9.1	1.4	6.5
8l	Pr	F	F	H	23.3	2.8	8.3
8m	Pr	F	F	F	37.0	4.1	9
6d[b]	na	na	na	na	1.85	<0.01	>185
PPT	na	na	na	na	10.1	0.5	20.2
E2	na	na	na	na	100	100	1

[a]HAP assay: mean value of independent determinations in duplicate. Results are reproducible within ±20%. na: not applicable. [b]For comparison, see refs 12 and 13.

8h, which were inactive at MCF-7/2a cells, activated the receptor in U2-OS/α cells with EC_{50} of 100 and 47 nM, respectively. Once again, the N-propyl derivatives were more active than their methyl-substituted analogues. Introduction of a 2-F substituent in the C2-aryl ring of **5c** increased the hormonal potency from EC_{50} = 0.4 nM to EC_{50} = 0.12 nM (**8b**). The same structural modification at C5 (**8d**) decreased the EC_{50} to 0.67 nM and at C3 (**8i**) to EC_{50} = 0.84 nM. The 2-Cl congener of **8d** was less active (**8h**, EC_{50} = 47 nM) and indicated the high importance of fluorine for the induction of transcriptional activity. Interestingly, it was impossible to strengthen the hormonal profile of the pyrroles by simultaneous F-substitution of the phenolic rings. **8b** is equipotent to PPT and the most potent compound in this transactivation assay.

Generally, the compounds were more active in U2-OS/α cells compared to MCF-7/2a cells (naturally containing ERα). For instance, **8b** displayed an EC_{50} in U2-OS/α cells (EC_{50} = 0.12 nM) comparable to that of PPT (0.1 nM). In MCF-7/2a cells, it was more than 20 times less active than in PPT (EC_{50} of 70 and 3 nM, respectively).

The reason for this finding is still unclear. However, it may be possible that the endogenous ERα signal cascade in MCF-7/2a cells might respond differently to various ligands. Another explanation could be that because of the overexpression of the ER in U2-OS cells, even very weak agonists such as **8g** and **8h** elicit a response.[23] Interestingly, the lack of activity in MCF-7/2a cells was also observed for imidazoles and other pyrroles with an analogue substitution pattern to **8g** and **8h**.[14,24]

All compounds demonstrated selectivity for ERα. In the experiments using U2-OS/β cells maximum IAs of about 15% were measured (Table 2). Compounds with an RBA higher than 10% at hERα resulted in EC_{50} values below 1 nM in U2-OS/α cells.

Inhibition of Cell Growth. The reduction of the IA at the highest concentration in the luciferase assay with MCF-7/2a cells induced us to examine if it was due to the inhibition of cell growth. All compounds were tested in hormone-dependent MCF-7 and hormone-independent MDA-MB-231 cells. The *N*-methyl derivatives showed very low cytotoxicity in MCF-7 cells (IC_{50} > 20 μM; see Table S1) comparable to that of PPT (IC_{50} = 27.2 μM). Elongation of the *N*-alkyl chain and introduction of fluorine substituents in the aromatic rings increased the cytoxic activity. 2,3,5-Tris(2-fluoro-4-hydroxyphenyl)-1-propyl-1*H*-pyrrole **8m** caused an IC_{50} of 5.6 μM very similar to that of E2. This fact and the growth inhibitory effects in the hormone-independent MDA-MB-231 cell line point to an unspecific cytotoxicity. Nevertheless the tested type B pyrroles influence the growth of the MCF-7 cells to a lesser extent than E2 or DES. For instance, none of the compounds stimulate the proliferation of the MCF-7 cells in low concentrations (an example for **8m**, **8k** is given in Figure S4).

3D Modeling and Structure−Activity Relationships (SARs). In order to rationalize the SAR of the series of compounds presented in this study, CCDCs software package GOLD[25] was used to dock compounds **8a−m** and PPT[11] into different crystal structures of ERα and ERβ. The resulting

dx.doi.org/10.1021/jm300860j | J. Med. Chem. 2012, 55, 9607−9618

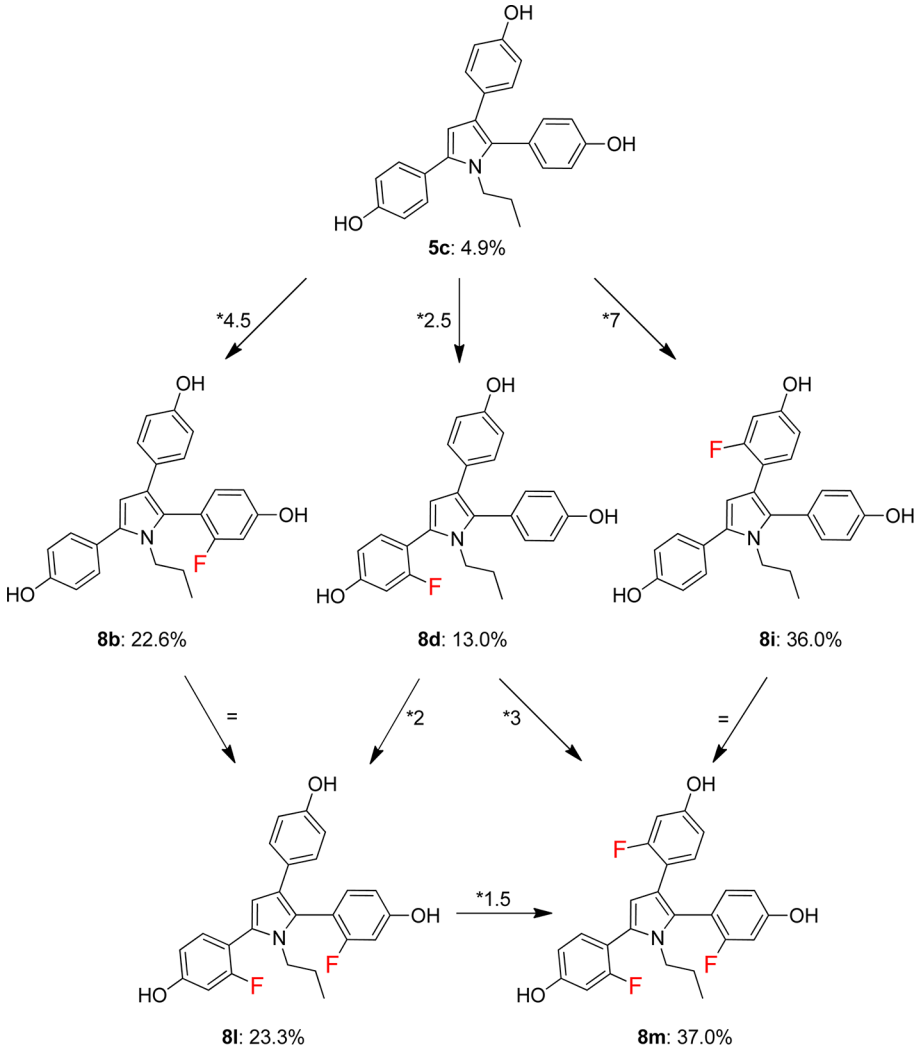

Figure 4. Comparison of the relative binding affinities of **5c** and F-substituted **8b**, **8d**, **8i**, **8l**, and **8m**.

binding poses were prioritized according to the proposed pharmacophore of PPT within ERα described previously.[11,13,33]

Our computational studies suggest that the R_1 alkyl substituent should not be too bulky, while the size affects selectivity: The propyl moiety at R_1 perfectly complements the cone-shaped cavity of ERα (as in the case of PPT),[11] while the narrower binding pocket of ERβ is limited to methyl substituents. Compounds **8a**–**m** are able to bind in orientations comparable to that of PPT (see Figures 7 and S5),[13] while no significant differences in orientation were observed. Overall, the *N*-propyl substituted compounds show higher activity on both estrogen receptor subtypes, mainly because of their increased lipophilicity (see above).

Fluorine substituents at R_2, R_3, and R_4 lead to an increase of activity (see above) at ERα because of increased lipophilic contact with the inner area of the estrogen receptor.

The binding mode of halogen-substituted pyrroles within ERα is ambiguous. While the pose presented in Figure S5 shows the binding pose analogue in Stauffer et al.,[11] docking experiments using different crystal structures (ERα, 2QZO[26] and 3L03;[29] ERβ, 2NV7,[30] 3OLL,[32] 3OLS[32]) revealed a different plausible binding mode. 2,3,5-Triaryl-1*H*-pyrroles have three hydroxyl groups in nearly equal distances, so six orientations in the LBD are possible, as shown in Figure 7.

Figure S5 illustrates representative docking poses for **8b**, **8f**, **8l** and PPT in ERα (PDB code 3ERD[28]). Our docking experiments show that binding mode C(5)′ is preferred in 3ERD: The hydroxyl group of the phenyl moiety at position 5 presumably forms hydrogen bonds to Glu353 and Arg394. We assume that the hydroxyl group in the aryl residue in C2 interacts with Met343 and His524 and the one in C3 with Gly521 and Met522. The fluorine substituent at R_3 may interact in a hydrogen-bond-like way with the nitrogen of Thr347, although the geometry for this interaction is not ideal and therefore not observed in the docking experiments.

An alternative possible orientation following the scheme of C(5) when docked into 3L03[29] is shown in Figure 8 (**8l** and **8m** as representative poses). The phenol moiety in position 5 shows hydrogen bonds with Glu353 and Arg394, while the phenol group at position 2 interacts with His524. In position 3 an interaction with the backbone at Met421 and Ile424 is formed corresponding to orientation C(5)′. The alkyl chain at R_3 interacts with the hydrophobic cavity consisting of Leu346, Thr347, Ala350, Trp383, Leu384, Leu387, and Leu540 (not all residues shown to improve clarity).

dx.doi.org/10.1021/jm300860j | *J. Med. Chem.* 2012, 55, 9607–9618

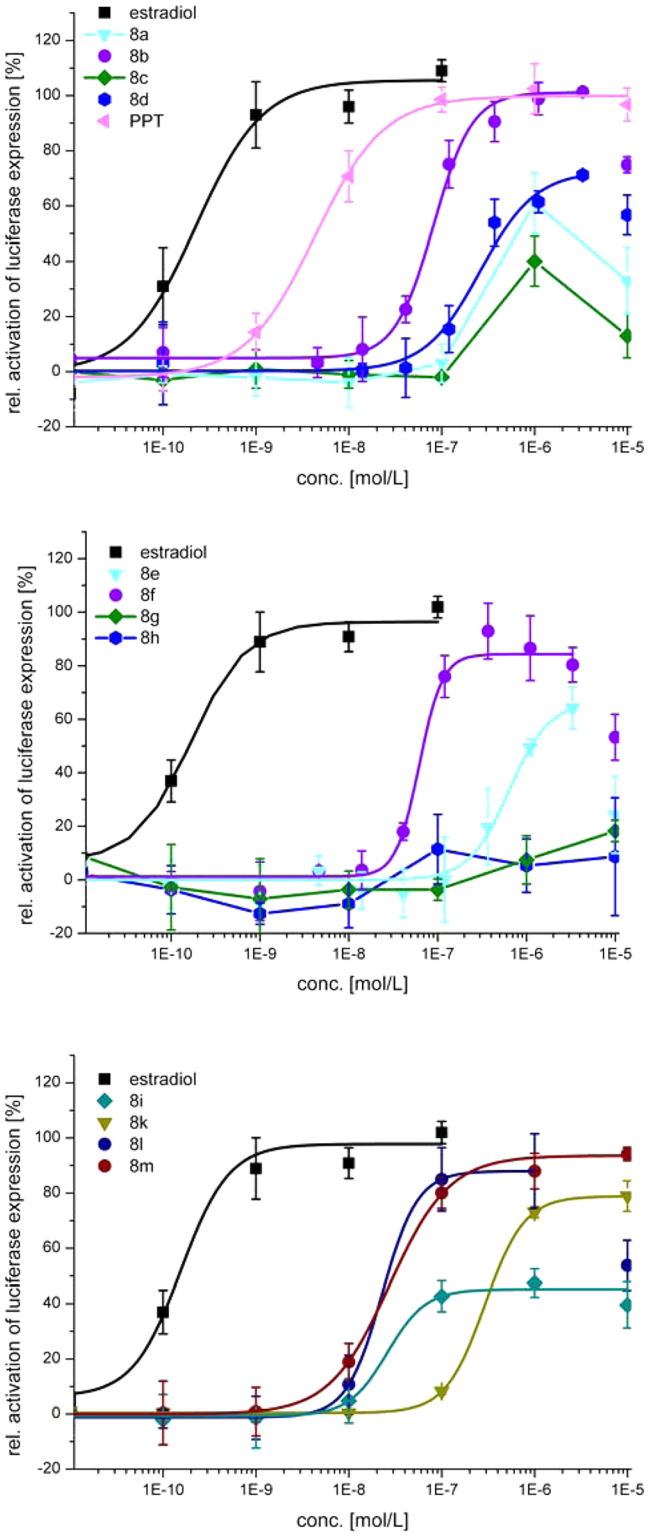

Figure 5. Top: Estrogenic activities of compounds **8a–d** and PPT in MCF-7/2a cells. Middle: Estrogenic activities of compounds **8e–h** in MCF-7/2a cells. Bottom: Estrogenic activities of compounds **8i–m** in MCF-7/2a cells. Diagrams show mean ± SD of a single representative experiment performed in quadruplicate, with estradiol graph included for comparison.

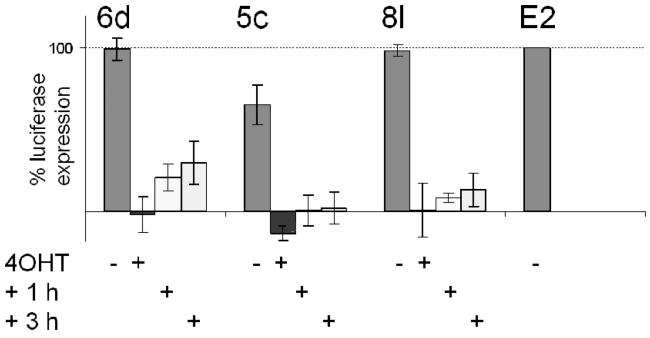

Figure 6. Co-incubation of **6d**, **5c**, or **8l** (1 μM) with 4-OHT (0.1 μM) in MCF-7/2a cells. Shown are mean values of two independent determinations, each performed in quadruplicate, ±SD. Control is vehicle, with 0% relative luciferase expression. Compounds (1 μM) were added to the cells without or simultaneously with 4-OHT or at 1 and 3 h before administration of 4-OHT.

DISCUSSION

In continuation of our recently published SAR studies, we tried to optimize the ER binding of 2,3,5-tris(4-hydroxyphenyl)-substituted pyrroles. At isolated receptors, the relative binding affinity to ERα and ERβ increased if halides are substituted in the ortho-position of the phenolic rings. Contrary to our earlier studies with hexestrol derivatives (e.g., 1,2-diamino-1,2-diarylethanes,[34] 2,3-diarylpiperazines,[35] and 4,5-diaryl-2-imidazolines),[36] in the class of type B pyrroles fluorine substituents caused a higher binding affinity than chlorine substituents. In the competition experiment with hERα the highest RBA values were obtained with R_4 = F (the influence of F-substitution is summarized in Figure 4). The ERα/ERβ ratio of all compounds was in the range 2–9.

Of high importance is the finding that the RBA values do not reflect the situation in cellular systems. Especially the ER selectivity is increased in cells. All 2,3,5-triarylpyrroles showed transactivation exclusively at ERα if the receptor is expressed in U2-OS cells. In the same experiment with ERβ no gene activation was determined. An explanation cannot be given at the moment. But it is well-known that for transcriptional activity a complex machinery has to be started. After ligand binding and receptor dimerization, the dimers translocate into the nucleus and bind to specific DNA sequences, the estrogen response elements. Then the binding of co-regulators starts the gene transcription. We assume that the binding of pyrroles to ERβ either caused a conformation that is not suitable for dimerization or prevented co-regulator binding. Especially the latter will be part of a new SAR study.

2,3,5-Triarylpyrroles caused growth inhibitory effects in tumor cells. The effect is observed in hormone-dependent MCF-7 as well as in MDA-MB-231 cells, so we assume an unselective mode of action. All compounds reduced the cell growth in MCF-7 cells to a lesser extent than DES and E2. Some of the compounds are even less cytotoxic than PPT. All 2,3,5-triarylpyrroles did not stimulate the cell growth in low concentration but influence the ERα content. The hormonally most active compounds **8m** and **8l** were also potent ER down-regulators in MCF-7 cells. In this case the growth stimulating ER system was destabilized causing reduced cell growth. As a consequence, **8m** and **8l** were more cytotoxic in hormone-dependent MCF 7 cells (IC_{50} = 5.6 and 8.0 μM, Table S1) than against hormone-independent MDA-MB-231 cells (IC_{50} = 21.9 and 20.9 μM, Table S1)

dx.doi.org/10.1021/jm300860j | J. Med. Chem. 2012, 55, 9607–9618

Table 2. Estrogenic Properties of 5c, 6d, 8a−m, PPT, and E2 in MCF-7/2a, U2-OS/α, and β Cells

					MCF-7/2a cells		U2-OS/α cells		U2-OS/β cells	
compd	R_1	R_2	R_3	R_4	IA (%)	EC_{50} [a] (nM)	IA (%)	EC_{50} [a] (nM)	IA (%)	EC_{50} [a] (nM)
5c	Pr	H	H	H	65 ± 12	50	55	0.4	16	
8a	Me	H	F	H	61 ± 11		101	60	12	
8b	Pr	H	F	H	101 ± 1	70	72	0.12	16	
8c	Me	F	H	H	40 ± 9		86	24	15	
8d	Pr	F	H	H	71 ± 1	240	91	0.67	15	
8e	Me	H	Cl	H	64 ± 7	600	97	16	12	
8f	Pr	H	Cl	H	92 ± 10	63	87	0.31	10	
8g	Me	Cl	H	H	0		46	100	26	
8h	Pr	Cl	H	H	0		79	47	13	
8i	Pr	H	H	F	50 ± 7	26	105[c]	0.84	0	
8k	Me	F	F	H	78 ± 5	290	110	15	5	
8l	Pr	F	F	H	88 ± 14	30	107	0.27	12	
8m	Pr	F	F	F	94 ± 2	23	100[c]	0.2	0	
6d[b]	na	na	na	na	99 ± 18	70	111	1.6	0	
PPT	na	na	na	na	97 ± 6	3	119	0.1	5	
E2	na	na	na	na	100	0.1	100	0.004	100	0.01

[a] EC_{50} values of compounds: for MCF-7/2a cells, mean values of three independent determinations, each performed in quadruplicate, ±SD; for U2-OS cells, mean values of three independent determinations, SD < 20%. na: not applicable. IA: intrinsic activity. [b] For comparison, see refs 12 and 13. For structural formulas, see Table 1. [c] IA: intrinsic activity at 1 μM.

EXPERIMENTAL SECTION

General. Melting points were determined on a Büchi B-545 and are uncorrected. NMR spectra were obtained with an Avance/DPX 400 (Bruker, Karlsruhe) 400 MHz spectrometer. Chemical shifts (δ) are reported in parts per million downfield from tetramethylsilane and referenced from solvent references. All aromatic d are "apparent" doublets. Electron impact (EI, 70 eV) mass spectra were obtained on a CH-7A (Varian MAT, Bremen) mass spectrometer. IR spectroscopy was performed on an ATI Mattson Genesis (Wigan, GB, KBr disks) or a Perkin-Elmer Spectrum 100. The elemental compositions of the compounds **8a−m** agreed to within ±0.4% of the calculated values (Vario EL, Elementar, Hanau). HPLC studies confirmed purity of compounds **8a−m** to be between 95% and 100% (Bio-Tek Kontron Instruments, Neufahrn). Chromatographic separations were performed on silica gel (Kieselgel 60, 0.063−0.100 mm; VWR, Bruchsal) columns by flash chromatography. Reactions were followed by thin-layer chromatography (TLC) on Merck aluminum silica gel (60 F_{254}) sheets that were visualized under a UV lamp.

Molecular Modeling and Docking Studies. Initial 3D coordinates of the compounds were generated using the software CORINA[37] by Molecular Networks (Erlangen, Germany) and subsequently docked using GOLD,[25] version 4.11 (CCDC, U.K.). Ensemble docking of compounds **8a−m**, PPT, and E2 was conducted using PDB complexes 3DT3,[27] 3ERD,[28] 3L03,[29] 2QZO[26] (for ERα), and 2NV7,[30] 2QTU,[31] 3OLL,[32] 3OLS,[32] (for ERβ). For pose ranking the PPT 3D pharmacophore was used in an analogue way as in a previous study,[38] following the already known 3D pharmacophore pattern of PPT. Pharmacophore creation and visualization were performed using the program LigandScout 3.02.[39−41]

Chemistry. General Method for Ether Cleavage (Method g, Scheme 2). The respective 1,3,5-tris(4-methoxyphenyl)-1*H*-pyrrole (**8a−m**) was dissolved in 15 mL of dry DCM under inert gas and cooled to 0 °C. BBr_3 dissolved in DCM (5 mL) was added slowly and the reaction mixture stirred overnight at room temperature. After evaporation of the solvent, redissolving several times in MeOH, purification of the residue was performed on silica gel by column chromatography using DCM/MeOH (9:1).

2-(2-Fluoro-4-hydroxyphenyl)-3,5-bis(4-hydroxyphenyl)-1-methyl-1*H*-pyrrole (8a). **8a** was produced from 2-(2-fluoro-4-methoxyphenyl)-3,5-bis(4-methoxyphenyl)-1-methyl-1*H*-pyrrole (**7a**), 0.84 mmol (352 mg), and BBr_3, 4.2 mmol (1056 mg). Brown solid, mp 158 °C. Yield: 0.28 mmol (106 mg), 34%. ^{1}H NMR (DMSO-d_6): δ = 10.05 (s, 1H, O*H*), 9.55 (s, 1H, O*H*), 9.14 (s, 1H, O*H*), 7.30 (d, 2H, *J* = 8.6, Ar*H*), 7.07 (t, 1H, *J* = 8.8, Ar*H*), 6.94 (d, 2H, *J* = 8.6, Ar*H*), 6.84 (d, 2H, *J* = 8.6, Ar*H*), 6.65 (m, 2H, Ar*H*), 6.57 (d, 2H, *J* = 8.7, Ar*H*), 6.26 (s, 1H, C*H*), 3.28 (s, 3H, NCH_3). Anal. ($C_{23}H_{18}FNO_3 \cdot 1.6H_2O$) C, H, N.

2-(2-Fluoro-4-hydroxyphenyl)-3,5-bis(4-hydroxyphenyl)-1-propyl-1*H*-pyrrole (8b). **8b** was produced from 2-(2-fluoro-4-methoxyphenyl)-3,5-bis(4-methoxyphenyl)-1-propyl-1*H*-pyrrole (**7b**), 0.40 mmol (178 mg), and BBr_3, 2.0 mmol (500 mg). Brown solid, mp 106 °C. Yield: 0.31 mmol (126 mg), 71%. ^{1}H NMR (DMSO-d_6): δ = 10.14 (s, 1H, O*H*), 9.59 (s, 1H, O*H*), 9.17 (s, 1H, O*H*), 7.31 (d, 2H, *J* = 8.6, Ar*H*), 7.16 (t, 1H, *J* = 8.8, Ar*H*), 6.99 (d, 2H, *J* = 8.6, Ar*H*), 6.89 (d, 2H, *J* = 8.5, Ar*H*), 6.71 (m, 2H, Ar*H*), 6.62 (d, 2H, *J* = 8.6, Ar*H*), 6.28 (s, 1H, C*H*), 3.70 (m, 2H, NCH_2CH$_2$CH$_3$), 1.24 (m, 2H, NCH$_2$CH_2CH$_3$), 0.52 (t, 3H, *J* = 7.4, NCH$_2$CH$_2$CH_3). Anal. ($C_{25}H_{22}FNO_3 \cdot 2H_2O$) C, H, N.

5-(2-Fluoro-4-hydroxyphenyl)-2,3-bis(4-hydroxyphenyl)-1-methyl-1*H*-pyrrole (8c). **8c** was produced from 5-(2-fluoro-4-methoxyphenyl)-2,3-bis(4-methoxyphenyl)-1-methyl-1*H*-pyrrole (**7c**), 0.72 mmol (300 mg), and BBr_3, 3.59 mmol (900 mg). Brown solid, mp 137 °C. Yield: 0.59 mmol (220 mg), 82%. ^{1}H NMR (DMSO-d_6): δ = 10.07 (s, 1H, O*H*), 9.58 (s, 1H, O*H*), 9.12 (s, 1H, O*H*), 7.27 (t, 1H, *J* = 8.9, Ar*H*), 7.09 (d, 2H, *J* = 8.6, Ar*H*), 6.93 (d, 2H, *J* = 8.6, Ar*H*), 6.80 (d, 2H, *J* = 8.6, Ar*H*), 6.70 (m, 2H, Ar*H*), 6.56 (d, 2H, *J* = 8.7, Ar*H*), 6.22 (s, 1H, C*H*), 3.20 (s, 3H, NCH_3). Anal. ($C_{23}H_{18}FNO_3 \cdot 1.3H_2O$) C, H, N.

5-(2-Fluoro-4-hydroxyphenyl)-2,3-bis(4-hydroxyphenyl)-1-propyl-1*H*-pyrrole (8d). **8d** was produced from 5-(2-fluoro-4-methoxyphenyl)-2,3-bis(4-methoxyphenyl)-1-propyl-1*H*-pyrrole (**7d**), 0.44 mmol (194 mg), and BBr_3, 2.2 mmol (554 mg). Brown solid, mp 100 °C. Yield: 0.22 mmol (90 mg), 50%. ^{1}H NMR (DMSO-d_6): δ = 9.80 (s, 1H, O*H*), 9.32 (s, 1H, O*H*), 8.84 (s, 1H, O*H*), 7.00 (t, 1H, *J* = 8.7, Ar*H*), 6.84 (d, 2H, *J* = 8.5, Ar*H*), 6.67 (d, 2H, *J* = 8.7, Ar*H*), 6.56 (d, 2H, *J* = 8.6, Ar*H*), 6.44 (m, 2H, Ar*H*), 6.30 (d, 2H, *J* = 8.7, Ar*H*), 5.94 (s, 1H, C*H*), 3.34 (t, 2H, *J* = 7.2, NCH_2CH$_2$CH$_3$), 0.89 (sextet, 2H, *J* = 7.6, NCH$_2$CH_2CH$_3$), 0.18 (t, 3H, *J* = 7.4, NCH$_2$CH$_2$CH_3). Anal. ($C_{25}H_{22}FNO_3 \cdot 1.3H_2O$) C, H, N.

2-(2-Chloro-4-hydroxyphenyl)-3,5-bis(4-hydroxyphenyl)-1-methyl-1*H*-pyrrole (8e). **8e** was produced from 2-(2-chloro-4-methoxyphenyl)-3,5-bis(4-methoxyphenyl)-1-methyl-1*H*-pyrrole (**7e**), 0.67 mmol (291 mg), and BBr_3, 3.4 mmol (840 mg). Orange solid, mp 105 °C. Yield: 0.33 mmol (128 mg), 49%. ^{1}H NMR (DMSO-d_6): δ = 10.10 (s, 1H, O*H*), 9.53 (s, 1H, O*H*), 9.11 (s, 1H, O*H*), 7.30 (d, 2H, *J* = 8.6, Ar*H*), 7.14 (d, 1H, *J* = 8.4, Ar*H*), 6.99 (d, 1H, *J* = 2.4, Ar*H*), 6.92 (d, 2H, *J* = 8.6, Ar*H*), 6.85 (d, 2H, *J* = 8.6, Ar*H*), 6.79 (dd, 1H, *J* = 8.4, *J*

dx.doi.org/10.1021/jm300860j | J. Med. Chem. 2012, 55, 9607−9618

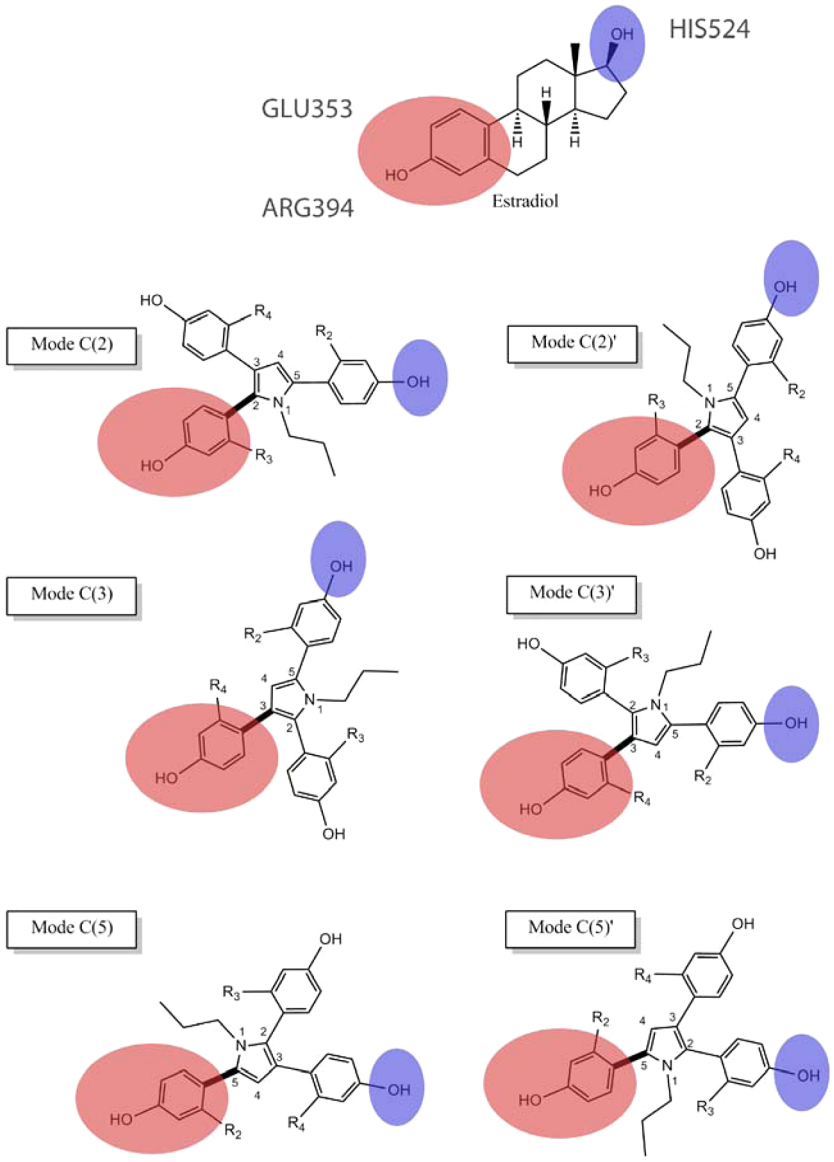

Figure 7. Potential 2,3,5-triaryl-1*H*-pyrroles binding modes relative to E2 as 2D projection, oriented to project into the estradiol A-ring binding pocket (red circle; Glu353, Arg394) while interacting with His524 (blue circle). By rotation of the pyrrole core around the lateral axis (darkened bond), modes C and C′ are related to each other.[11]

= 2.5, Ar*H*), 6.57 (d, 2H, *J* = 8.7, Ar*H*),6.28 (s, 1H, C*H*), 3.24 (s, 3H, NCH_3). Anal. ($C_{23}H_{18}ClNO_3 \cdot 1.3H_2O$) C, H, N.

2-(2-Chloro-4-hydroxyphenyl)-3,5-bis(4-hydroxyphenyl)-1-propyl-1*H*-pyrrole (8f). **8f** was produced from 2-(2-chloro-4-methoxyphenyl)-3,5-bis(4-methoxyphenyl)-1-propyl-1*H*-pyrrole (**7f**), 0.44 mmol (220 mg), and BBr_3, 2.1 mmol (550 mg). Orange solid, mp 102 °C. Yield: 0.17 mmol (70 mg), 38%. ^{1}H NMR (DMSO-d_6): δ = 10.09 (s, 1H, O*H*), 9.52 (s, 1H, O*H*), 9.09 (s, 1H, O*H*), 7.25 (d, 2H, *J* = 8.5, Ar*H*), 7.17 (d, 1H, *J* = 8.4, Ar*H*), 6.95 (d, 1H, *J* = 2.4, Ar*H*), 6.89 (d, 2H, *J* = 8.6, Ar*H*), 6.83 (d, 2H, *J* = 8.6, Ar*H*), 6.80 (dd, 1H, *J* = 8.4, *J* = 2.5, Ar*H*), 6.55 (d, 2H, *J* = 8.6, Ar*H*), 6.22 (s, 1H, C*H*), 3.60 (m, 2H, NCH_2CH$_2$CH$_3$), 1.17 (m, 2H, NCH$_2$CH_2CH$_3$), 0.46 (t, 3H, *J* = 7.4, NCH$_2$CH$_2$CH_3). Anal. ($C_{25}H_{22}ClNO_3 \cdot 1.1H_2O$) C, H, N.

5-(2-Chloro-4-hydroxyphenyl)-2,3-bis(4-hydroxyphenyl)-1-methyl-1*H*-pyrrole (8g). **8g** was produced from 5-(2-chloro-4-methoxyphenyl)-2,3-bis(4-methoxyphenyl)-1-methyl-1*H*-pyrrole (**7g**), 0.45 mmol (195 mg), and BBr_3, 2.2 mmol (563 mg). Orange solid, mp 142 °C. Yield: 0.26 mmol (100 mg), 57%. ^{1}H NMR (DMSO-d_6): δ = 10.07 (s, 1H, O*H*), 9.57 (s, 1H, O*H*), 9.11 (s, 1H, O*H*), 7.29 (d, 1H, *J* = 8.4, Ar*H*), 7.09 (d, 2H, *J* = 8.5, Ar*H*), 6.94 (m, 3H, Ar*H*), 6.81 (m, 3H, Ar*H*), 6.56 (d, 2H, *J* = 8.6, Ar*H*), 6.19 (s, 1H, C*H*), 3.13 (s, 3H, NCH_3). Anal. ($C_{23}H_{18}ClNO_3 \cdot 1H_2O$) C, H, N.

5-(2-Chloro-4-hydroxyphenyl)-2,3-bis(4-hydroxyphenyl)-1-propyl-1*H*-pyrrole (8h). **8h** was produced from 5-(2-chloro-4-methoxyphenyl)-2,3-bis(4-methoxyphenyl)-1-propyl-1*H*-pyrrole (**7h**), 0.65 mmol (300 mg), and BBr_3, 3.2 mmol (813 mg). After flash chromatography, the compound is purified further by MPLC. Orange solid, mp 123 °C. Yield: 0.05 mmol (20 mg), 7%. ^{1}H NMR (DMSO-d_6): δ = 10.06 (s, 1H, O*H*), 9.58 (s, 1H, O*H*), 9.09 (s, 1H, O*H*), 7.29 (d, 1H, *J* = 8.4, Ar*H*), 7.07 (d, 2H, *J* = 8.5, Ar*H*), 6.94 (d, 1H, *J* = 2.4, Ar*H*), 6.92 (d, 2H, *J* = 8.6, Ar*H*), 6.82 (m, 3H, Ar*H*), 6.54 (d, 2H, *J* = 8.7, Ar*H*), 6.16 (s, 1H, C*H*), 3.53 (t, 2H, *J* = 7.6, NCH_2CH$_2$CH$_3$), 1.11 (sextet, 2H, *J* = 7.4, NCH$_2$CH_2CH$_3$), 0.41 (t, 3H, *J* = 7.4, NCH$_2$CH$_2$CH_3). Anal. ($C_{25}H_{22}ClNO_3 \cdot 1.5H_2O$) C, H, N.

3-(2-Fluoro-4-hydroxyphenyl)-2,5-bis(4-hydroxyphenyl)-1-propyl-1*H*-pyrrole (8i). **8i** was produced from 3-(2-fluoro-4-methoxyphenyl)-2,5-bis(4-methoxyphenyl)-1-propyl-1*H*-pyrrole (**7i**), 0.22 mmol (100 mg), and BBr_3, 1.0 mmol (253 mg). Yellow solid, mp 201 °C. Yield: 0.13 mmol (53 mg), 60%. ^{1}H NMR (DMSO-d_6): δ = 9.58 (s, 1H, O*H*), 9.51 (s, 1H, O*H*), 9.50 (s, 1H, O*H*), 7.26 (d, *J* = 8.4, 2H, Ar*H*), 7.04 (d, *J* = 8.4, 2H, Ar*H*), 6.79 (m, 5H, Ar*H*), 6.42 (dd, *J* =

dx.doi.org/10.1021/jm300860j | *J. Med. Chem.* 2012, 55, 9607−9618

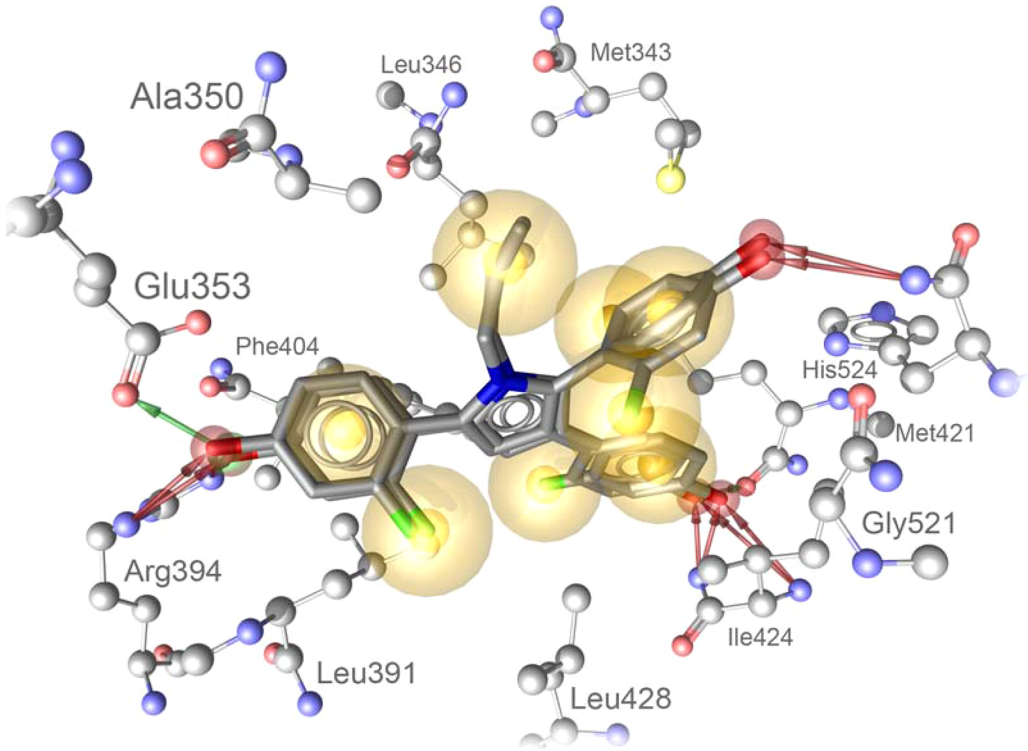

Figure 8. Presumed upside-down poses of **8l** and **8m** inside the cavity of ERα (PDB code 3L03[23]). Hydrogen bonds are shown as green and red arrows, and lipophilic features are shown as yellow spheres. Font size for amino acid labels corresponds to position on the *z*-axis (depth).

26.4, 2.2, 1H, Ar*H*), 6.39 (dd, *J* = 22.6, 2.2, 1H, Ar*H*), 6.10 (d, *J* = 1.9, 1H, C*H*), 3.78 (t, *J* = 7.3, 2H, NCH_2CH$_2$CH$_3$), 1.15 (m, 2H, NCH$_2$CH_2CH$_3$), 0.42 (t, *J* = 7.4, 3H, NCH$_2$CH$_2$CH_3). Anal. ($C_{25}H_{22}FNO_3 \cdot 1H_2O$) C, H, N.

2,5-Bis(2-fluoro-4-hydroxyphenyl)-3-(4-hydroxyphenyl)-1-methyl-1*H*-pyrrole (8k). **8k** was produced from 2,5-bis(2-fluoro-4-methoxyphenyl)-3-(4-methoxyphenyl)-1-methyl-1*H*-pyrrole (**7k**), 1.6 mmol (700 mg), and BBr_3, 8.0 mmol (2010 mg). Orange solid, mp 126 °C. Yield: 0.89 mmol (350 mg), 55%. ^{1}H NMR (DMSO-d_6): δ = 10.10 (s, 1H, O*H*), 10.07 (s, 1H, O*H*), 9.14 (s, 1H, O*H*) 7.27 (t, 1H, *J* = 8.8, Ar*H*), 7.06 (t, 1H, *J* = 8.8, Ar*H*), 6.94 (d, 2H, *J* = 8.5, Ar*H*), 6.69 (m, 4H, Ar*H*), 6.58 (d, 2H, *J* = 8.6, Ar*H*), 6.27 (s, 1H, C*H*), 3.16 (s, 3H, NCH_3). Anal. ($C_{23}H_{17}F_2NO_3 \cdot 1.3H_2O$) C, H, N.

2,5-Bis(2-fluoro-4-hydroxyphenyl)-3-(4-hydroxyphenyl)-1-propyl-1*H*-pyrrole (8l). **8l** was produced from 2,5-bis(2-fluoro-4-methoxyphenyl)-3-(4-methoxyphenyl)-1-propyl-1*H*-pyrrole (**7l**), 0.86 mmol (400 mg), and BBr_3, 4.3 mmol (1080 mg). Orange solid, mp 115 °C. Yield: 0.83 mmol (350 mg), 96%. ^{1}H NMR (DMSO-d_6): δ = 10.18 (s, 1H, O*H*), 10.15 (s, 1H, O*H*), 9.21 (s, 1H, O*H*), 7.32 (t, 1H, *J* = 8.6, Ar*H*), 7.17 (t, 1H, *J* = 8.8, Ar*H*), 7.01 (d, 2H, *J* = 8.5, Ar*H*), 6.76 (m, 4H, Ar*H*), 6.65 (m, 2H, *J* = 8.6, Ar*H*), 6.33 (s, 1H, C*H*), 3.61 (m, 2H, NCH_2CH$_2$CH$_3$), 1.23 (sextet, 2H, *J* = 7,2, NCH$_2$CH_2CH$_3$), 0.53 (t, 3H, *J* = 7.4, NCH$_2$CH$_2$CH_3). Anal. ($C_{25}H_{21}F_2NO_3 \cdot 1.5H_2O$) C, H, N.

2,3,5-Tris(2-fluoro-4-hydroxyphenyl)-1-propyl-1*H*-pyrrole (8m). **8m** was produced from 2,3,5-tris(2-fluoro-4-methoxyphenyl)-1-propyl-1*H*-pyrrole (**7m**), 0.15 mmol (72 mg), and BBr_3, 0.67 mmol (169 mg). Yellow solid, mp 105 °C. Yield: 0.06 mmol (26 mg), 40%. ^{1}H NMR (DMSO-d_6): δ = 10.10 (s, 1H, O*H*), 10.07 (s, 1H, O*H*), 9.66 (s, 1H, O*H*), 7.24 (d, 1H, *J* = 8.7, Ar*H*), 7.01 (d, 1H, *J* = 8.7, Ar*H*), 6.82 (d, 1H, *J* = 8.8, Ar*H*), 6.66 (m, 4H, Ar*H*), 6.43 (m, 2H, Ar*H*), 6.17 (d, 1H, *J* = 1.8, C*H*), 3.59 (m, 2H, NCH_2CH$_2$CH$_3$), 1.14 (m, 2H, *J* = 7.3, NCH$_2$CH_2CH$_3$), 0.43 (t, 3H, *J* = 7.4, NCH$_2$CH$_2$CH_3). Anal. ($C_{25}H_{20}F_3NO_3 \cdot 1H_2O$) C, H, N.

Stability Studies. The following was used: HPLC, Bio-Tek Kontron Instruments, Germany; C18 reverse phase column, Eurospher 100-5 C18, 250 mm × 4 mm, Knauer GmbH, Germany. HPLC conditions were the following: methanol/H_2O, 7/3; isocratic elution; detection wavelength, 265 nm; flow rate, 0.8 mL/min; run time, 20 min. Compounds were dissolved in methanol (10^{-2} M) and diluted with PBS to a final concentration of 10^{-5} M. Compounds were kept at 37 °C and were measured once directly after dissolving and six more times during the following 195 h.

Cell Lines and Growth Conditions. MCF-7/2a cells, MCF-7 cells, and MDA-MB-231 cells were maintained as a monolayer culture at 37 °C in a humidified atmosphere (95% air, 5% CO_2) in T-25 flasks. U2-OS cells were maintained as a monolayer culture at 37 °C in humidified atmosphere (92.5% air, 7.5% CO_2) in T-25 flasks. Growth medium for MCF-7/2a cells consisted of phenol red free DMEM high glucose with sodium pyruvate (110 mg/L), ct-FCS 5%, and Geneticin solution, 0.5%. Growth medium for U2-OS, MCF-7, and MDA-MB-231 cells consisted of L-glutamine and sodium pyruvate containing DMEM high glucose with FCS, 5%.

Estrogenic Activity. Luciferase Assay (MCF-7/2a Cells). Four days before starting the experiment MCF-7/2a cells were cultivated in DMEM supplemented with dextran−charcoal-treated FCS (ct-FCS, 50 mL/L). Cells from an 80% confluent monolayer were removed by trypsinization and suspended to approximately 10^5 cells/mL in the growth medium mentioned above. The cell suspension was then cultivated in 96-well flat-bottomed plates at growing conditions (see above). After 24 h, the test compounds were added to achieve concentrations ranging from 10^{-5} to 10^{-11} M (estradiol from 10^{-7} to 10^{-13} M), and the plates were incubated for 50 h. Subsequently, 50 μL of cell culture lysis reagent was added to each well. After 30 min of lysis at room temperature, an amount of 50 μL of the Promega luciferase assay reagent (Promega, Mannheim, Germany) was added. Luminescence (in relative light unit, RLU) was measured for 10 s using a luminometer. Estrogenic activity was expressed as percent activation of a 3×10^{-9} M estradiol control (100%).

Luciferase Assay (U2-OS Cells). U2-OS cells were transferred to DMEM supplemented with dextran−charcoal-treated FCS 24 h before the experiment. Cells from an almost confluent monolayer were split and seeded in 10 cm i.d. Petri dishes at 1×10^6 cells per dish at least 24 h prior to transfection. Transient transfection of the cells with 0.05 μg of receptor plasmid pSG5-ERα or pSG5-ERβ FL and 5 μg of the reporter plasmid p(ERE)$_2$-luc$^+$ was carried out after 6 h using 15 μL of

dx.doi.org/10.1021/jm300860j | *J. Med. Chem.* 2012, 55, 9607−9618

FuGENE 6 (Roche Diagnostics, Mannheim, Germany) according to the manufacturer's instructions. After 18 h the cells were washed with PBS and harvested by trypsinization and seeded in white 96-well plates at 10^4 cells/well in 100 μL of ct-DMEM. After 3 h, the medium was replaced by medium containing either E2 or test compounds in final concentrations ranging from 0.1 pM to 10 nM (E2) or 0.1 nM to 10 mM (test compounds). After 18 h of incubation, the medium was removed and cells were lyzed and luciferase activity assayed as described above.

Ability of Compounds To Regulate ERα Levels in MCF-7 Cells. MCF-7 cells are plated in six-well plates (500 000 cells per well) containing ct-DMEM. After 24 h of culture, medium is removed and cells are exposed to increasing amounts of the investigated compounds for 24 h in a fresh medium; control cells are maintained in culture without any compound. Cells are then washed with Tris buffered saline (50 mM Tris, pH 7.5, 150 mM NaCl) and lysed for 30 min at 4 °C in radioimmunoprecipitation assay buffer. ERα levels in these lysates were finally assessed by Western blotting following a procedure described in ref 42. Briefly, ERα is detected with a mouse monoclonal antibody (F-10, Santa Cruz Biotechnology, Santa Cruz, CA). Actin, used as a loading control, is detected with mouse monoclonal antibody MAB1501R from Millipore. Exposure to primary antibodies is followed by incubation in the presence of a horseradish peroxidase-conjugated goat anti-mouse secondary antibody (Pierce, Rockford, IL). Peroxidase activity is revealed with Supersignal West Pico chemiluminescent substrate from Pierce. ERα and actin bands are captured with a CCD camera.

Recombinant ERα/ERβ (HAP Assay). An ethanolic solution (250 fmol/μL) of recombinant human estrogen receptor (hERα or hERβ, Calbiochem) was diluted with Tris-HCl buffer, pH 8.0 (1:100). These hERα or hERβ preparations adsorbed on hydroxyl apatite pellets (prepared in 10 mmol/L of Tris-HCl buffer, pH 8.0, containing 1 mg/mL BSA) which were labeled with increasing concentrations of the test compound (10^{-10}–10^{-5} M) and [^{3}H]E2 (5 nM, Perkin-Elmer) and were incubated for 3 h at room temperature. Bond [^{3}H]E2 was then successively extracted with ethanol, and aliquots of 200 μL of the ethanolic extracts were transferred to scintillation vials containing 3.5 mL of scintillator Ecoscint H (National Diagnostics, Atlanta, GA) for radioactivity counting. All measurements were performed in duplicate. The results (relative radioactivity) were expressed as percentage of a solvent treated control sample. Relative concentrations of compounds required to reduce the binding of [^{3}H]E_2 by 50% gave their IC_{50} values. The relative binding affinity was calculated by dividing the IC_{50} of E2 by the IC_{50} of the respective compound. Binding affinities are expressed relative to estradiol (RBA(E2) = 100%).

Determination of Inhibition of Cell Growth in MCF-7 and MDA-MB-231 Human Breast Cancer Cells. Cells from an 80% confluent monolayer were harvested by trypsinization and suspended to approximately 10^4 (MCF-7 cells) or 7.5×10^3 cells/mL (MDA-MB-231 cells). At the beginning of the experiment, the cell suspension was transferred to 96-well microplates (100 μL/well). After their cultivation for 3 days at growing conditions, the test compounds dissolved in DMEM were added at final concentrations ranging from 3.13 to 50 μM. Control wells (16/plate) contained 0.1% of DMSO, which was used for the preparation of the stock solutions. The initial cell density was determined by addition of glutaric dialdehyde to one plate (1% in PBS, 100 μL/well). After incubation for 3 days (MDA-MB-231 cells) or 4 days (MCF-7 cells), the medium was removed and glutaric dialdehyde (1% in PBS, 100 μL/well) was added for fixation. After 30 min, the solution of the aldehyde was decanted and an amount of 150 μL of PBS/well was added. The plates were stored at 4 °C until staining. Cells were stained by treating them for 30 min with 100 μL of an aqueous solution of crystal violet (0.02%). After decanting, cells were washed several times with water to remove the adherent dye. After addition of 180 μL of ethanol (70%), plates were gently shaken for 3–4 h. Optical density of each well was measured in a microplate autoreader at 590 nm.

■ ASSOCIATED CONTENT

Ⓢ Supporting Information

Synthesis and analytical data of all precursors, additional spectroscopic data of target compounds **8a–m**, results from cytotoxicity tests, ER down-regulation, and binding pose from the molecular modeling. This material is available free of charge via the Internet at http://pubs.acs.org.

■ AUTHOR INFORMATION

Corresponding Author

*Phone: +43 512 507 58200. Fax: +43 512 507 58299. E-mail: ronald.gust@uibk.ac.at.

Notes

The authors declare no competing financial interest.

■ ACKNOWLEDGMENTS

The technical assistance of Silke Bergemann and Maxi Wenzel is acknowledged.

■ ABBREVIATIONS USED

E2, estradiol; (h)ER, (human) estrogen receptor; ERα, estrogen receptor alpha; ERβ, estrogen receptor β; PPT, propylpyrazole triol; TAM, tamoxifen; RAL, raloxifene; 4-OHT, 4-hydroxytamoxifen; HAP, hydroxyl apatite; MCF-7, Michigan Cancer Foundation 7; U2-OS, human osteosarcoma; [^{3}H]E2, tritium labeled estradiol; RBA, relative binding affinity; IA, intrinsic activity; MDA-MB-231, M. D. Anderson metastatic breast cancer; DMEM, Dulbecco's modified Eagle medium; ct, dextran-charcoal-treated; FCS, fetal calf serum; ERE, estrogen response element; DCM, dichloromethane; PBS, phosphate buffered saline; RLU, relative light unit

■ REFERENCES

(1) Silverman, S. L.; Christiansen, C.; Genant, H. K.; Vukicevic, S.; Zanchetta, J. R.; de Villiers, T. J.; Constantine, G. D.; Chines, A. A. Efficacy of bazedoxifene in reducing new vertebral fracture risk in postmenopausal women with osteoporosis: results from a 3-year, randomized, placebo-, and active-controlled clinical trial. *J. Bone Miner. Res.* **2008**, *23*, 1923–1934.

(2) Kawate, H.; Takayanagi, R. Efficacy and safety of bazedoxifene for postmenopausal osteoporosis. *Clin. Interventions Aging* **2011**, *6*, 151–160.

(3) Crabtree, J. S.; Peano, B. J.; Zhang, X.; Komm, B. S.; Winneker, R. C.; Harris, H. A. Activity of three selective estrogen receptor modulators on hormone-dependent responses in the mouse uterus and mammary gland. *Mol. Cell. Endocrinol.* **2008**, *287*, 40–46.

(4) Bardin, A.; Boulle, N.; Lazennec, G.; Vignon, F.; Pujol, P. Loss of ERbeta expression as a common step in estrogen-dependent tumor progression. *Endocr.-Relat. Cancer* **2004**, *11*, 537–551.

(5) Park, B.-W.; Kim, K.-S.; Heo, M.-K.; Ko, S.-S.; Lee, K. S.; Hong, S. W.; Yang, W.-I.; Kim, J.-H.; Kim, G. E. Expression of estrogen receptor-β in normal mammary and tumor tissues: Is it protective in breast carcinogenesis? *Breast Cancer Res. Treat.* **2003**, *80*, 79–85.

(6) Gustafsson, J.-Å.; Warner, M. Estrogen receptor β in the breast: role in estrogen responsiveness and development of breast cancer. *J. Steroid Biochem. Mol. Biol.* **2000**, *74*, 245–248.

(7) Speirs, V.; Skliris, G. P.; Burdall, S. E.; Carder, P. J. Distinct expression patterns of ERα and ERβ in normal human mammary gland. *J. Clin. Pathol.* **2002**, *55*, 371–374.

(8) Hayashi, S.-I.; Eguchi, H.; Tanimoto, K.; Yoshida, T.; Omoto, Y.; Inoue, A.; Yoshida, N.; Yamaguchi, Y. The expression and function of estrogen receptor alpha and beta in human breast cancer and its clinical application. *Endocr.-Relat. Cancer* **2003**, *10*, 193–202.

(9) Clarke, R. B.; Howell, A.; Potten, C. S.; Anderson, E. Dissociation between steroid receptor expression and cell proliferation in the human breast. *Cancer Res.* **1997**, *57*, 4987−4991.
(10) Fink, B. E.; Mortensen, D. S.; Stauffer, S. R.; Aron, Z. D.; Katzenellenbogen, J. A. Novel structural templates for estrogen-receptor ligands and prospects for combinatorial synthesis of estrogens. *Chem. Biol.* **1999**, *6*, 205−219.
(11) Stauffer, S. R.; Coletta, C. J.; Tedesco, R.; Nishiguchi, G.; Carlson, K.; Sun, J.; Katzenellenbogen, B. S.; Katzenellenbogen, J. A. Pyrazole ligands: structure−affinity/activity relationships and estrogen receptor alpha selective agonists. *J. Med. Chem.* **2000**, *43*, 4934−4947.
(12) Schäfer, A.; Wellner, A.; Gust, R. Synthesis and investigations on the oxidative degradation of C3/C5-alkyl-1,2,4-triarylpyrroles as ligands for the estrogen receptor. *ChemMedChem* **2011**, *6*, 794−803.
(13) Schäfer, A.; Wellner, A.; Strauss, M.; Wolber, G.; Gust, R. Development of 2,3,5-triaryl-1*H*-pyrroles as estrogen receptor alpha selective ligands. *ChemMedChem* **2011**, *6*, 2055−2062.
(14) Hoffmann, R. Synthese und Pharmakologische Untersuchung Neuer Triaryl-1H-pyrrole mit Estrogenen, Zytotoxischen und COX-Inhibitorischen Eigenschaften. Ph.D. Thesis. Freie Universität Berlin, Berlin, Germany, 2007.
(15) Mortensen, D. S.; Rodriguez, A. L.; Carlson, K. E.; Sun, J.; Katzenellenbogen, B. S.; Katzenellenbogen, J. A. Synthesis and biological evaluation of a novel series of furans: ligands selective for estrogen receptor alpha. *J. Med. Chem.* **2001**, *44*, 3838−3848.
(16) Wyvratt, J. M.; Hazen, G. G.; Weinstock, L. M. A convenient, general synthesis of alpha-trichloro-methyl carbinols. *J. Org. Chem.* **1987**, *52*, 944−945.
(17) Cafiero, L. R.; Snowden, T. S. General and practical conversion of aldehydes to homologated carboxylic acids. *Org. Lett.* **2008**, *10*, 3853−3856.
(18) Oki, M. *Applications of Dynamic NMR Spectroscopy to Organic Chemistry*; VCH Publishers: Deerfield Beach, FL, 1985; Vol. *4*, p 423.
(19) Oki, M. *The Chemistry of Rotational Isomers*; Springer: Berlin, Germany, 1993; Vol. *30*, p 172.
(20) Hafner, F.; Holler, E.; von Angerer, E. Effect of growth factors on estrogen receptor mediated gene expression. *J. Steroid Biochem. Mol. Biol.* **1996**, *58*, 385−393.
(21) Meyer, T.; Koop, R.; von Angerer, E.; Schönenberger, H.; Holler, E. A rapid luciferase transfection assay for transcription activation effects and stability control of estrogenic drugs in cell cultures. *J. Cancer Res. Clin. Oncol.* **1994**, *120*, 359−364.
(22) Laïos, I.; Cleeren, A.; Leclercq, G.; Nonclercq, D.; Laurent, G.; Schlenk, M.; Wellner, A.; Gust, R. Effects of (*R*,*S*)/(*S*,*R*)-4,5-bis(2-chloro-4-hydroxyphenyl)-2-imidazolines and (*R*,*S*)/(*S*,*R*)-2,3-bis(2-chloro-4-hydroxyphenyl)piperazines on estrogen receptor alpha level and transcriptional activity in MCF-7 cells. *Biochem. Pharmacol.* **2007**, *74*, 1029−1038.
(23) Watts, C. K. W.; King, R. J. B. Overexpression of estrogen receptor in HTB 96 human osteosarcoma cells results in estrogen-induced growth inhibition and receptor cross talk. *J. Bone Miner. Res.* **1994**, *9*, 1251−1258.
(24) Wiglenda, T.; Gust, R. Structure−activity relationship study to understand the estrogen receptor-dependent gene activation of aryl- and alkyl-substituted 1*H*-imidazoles. *J. Med. Chem.* **2007**, *50*, 1475−1484.
(25) Jones, G.; Willett, P.; Glen, R. C.; Leach, A. R.; Taylor, R. Development and validation of a genetic algorithm for flexible docking. *J. Mol. Biol.* **1997**, *267*, 727−748.
(26) Bruning, J. B.; Parent, A. A.; Gil, G.; Zhao, M.; Nowak, J.; Pace, M. C.; Smith, C. L.; Afonine, P. V.; Adams, P. D.; Katzenellenbogen, J. A.; Nettles, K. W. Coupling of receptor conformation and ligand orientation determine graded activity. *Nat. Chem. Biol.* **2010**, *6*, 837−843.
(27) Fang, J.; Akwabi-Ameyaw, A.; Britton, J. E.; Katamreddy, S. R.; Navas, F., 3rd; Miller, A. B.; Williams, S. P.; Gray, D. W.; Orband-Miller, L. A.; Shearin, J.; Heyer, D. Synthesis of 3-alkyl naphthalenes as novel estrogen receptor ligands. *Bioorg. Med. Chem. Lett.* **2008**, *18*, 5075−5077.
(28) Shiau, A. K.; Barstad, D.; Loria, P. M.; Cheng, L.; Kushner, P. J.; Agard, D. A.; Greene, G. L. The structural basis of estrogen receptor/coactivator recognition and the antagonism of this interaction by tamoxifen. *Cell* **1998**, *95*, 927−937.
(29) Rajan, S. S.; Kim, Y.; Vanek, K.; Joachimiak, A.; Greene, G. L. Crystal structure of human estrogen receptor alpha ligand-binding domain in complex with a glucocorticoid receptor interacting protein 1 nr box II peptide and estra-1,3,5(10)-triene-3,15 alpha,16alpha,17beta-tetrol. To be published.
(30) Mewshaw, R. E.; Bowen, S. M.; Harris, H. A.; Xu, Z. B.; Manas, E. S.; Cohn, S. T. ERbeta ligands. Part 5: synthesis and structure−activity relationships of a series of 4′-hydroxyphenyl-aryl-carbaldehyde oxime derivatives. *Bioorg. Med. Chem. Lett.* **2007**, *17*, 902−906.
(31) Richardson, T. I.; Dodge, J. A.; Wang, Y.; Durbin, J. D.; Krishnan, V.; Norman, B. H. Benzopyrans as selective estrogen receptor beta agonists (SERBAs). Part 5: Combined A- and C-ring structure−activity relationship studies. *Bioorg. Med. Chem. Lett.* **2007**, *17*, 5563−5566.
(32) Möcklinghoff, S.; Rose, R.; Carraz, M.; Visser, A.; Ottmann, C.; Brunsveld, L. Synthesis and crystal structure of a phosphorylated estrogen receptor ligand binding domain. *ChemBioChem* **2010**, *11*, 2251−2254.
(33) Stauffer, S. R.; Huang, Y.; Coletta, C. J.; Tedesco, R.; Katzenellenbogen, J. A. Estrogen pyrazoles: defining the pyrazole core structure and the orientation of substituents in the ligand binding pocket of the estrogen receptor. *Bioorg. Med. Chem.* **2001**, *9*, 141−150.
(34) Karl, J.; Gust, R.; Spruss, T.; Schneider, M. R.; Schoenenberger, H.; Engel, J.; Wrobel, K. H.; Lux, F.; Haeberlin, S. T. Ring-substituted [1,2-bis(4-hydroxyphenyl)ethylenediamine]dichloroplatinum(II) complexes: compounds with a selective effect on the hormone-dependent mammary carcinoma. *J. Med. Chem.* **1988**, *31*, 72−83.
(35) Gust, R.; Keilitz, R.; Schmidt, K. Synthesis, structural evaluation, and estrogen receptor interaction of 2,3-diarylpiperazines. *J. Med. Chem.* **2002**, *45*, 2325−2337.
(36) Gust, R.; Keilitz, R.; Schmidt, K.; von Rauch, M. (4*R*,5*S*)/(4*S*,5*R*)-4,5-Bis(4-hydroxyphenyl)-2-imidazolines: ligands for the estrogen receptor with a novel binding mode. *J. Med. Chem.* **2002**, *45*, 3356−3365.
(37) Sadowski, J.; Gasteiger, J.; Klebe, G. Comparison of automatic three-dimensional model builders using 639 X-ray structures. *J. Chem. Inf. Comput. Sci.* **1994**, *34*, 1000−1008.
(38) Goebel, M.; Wolber, G.; Markt, P.; Staels, B.; Unger, T.; Kintscher, U.; Gust, R. Characterization of new PPAR[gamma] agonists: benzimidazole derivatives—importance of positions 5 and 6, and computational studies on the binding mode. *Bioorg. Med. Chem.* **2010**, *18*, 5885−5895.
(39) Wolber, G.; Langer, T. LigandScout: 3-D pharmacophores derived from protein-bound ligands and their use as virtual screening filters. *J. Chem. Inf. Model.* **2005**, *45*, 160−169.
(40) Wolber, G.; Dornhofer, A. A.; Langer, T. Efficient overlay of small organic molecules using 3D pharmacophores. *J. Comput.-Aided Mol. Des.* **2006**, *20*, 773−788.
(41) Wolber, G.; Seidel, T.; Bendix, F.; Langer, T. Molecule-pharmacophore superpositioning and pattern matching in computational drug design. *Drug Discovery Today* **2008**, *13*, 23−29.
(42) El Khissiin, A.; Journe, F.; Laios, I.; Seo, H. S.; Leclercq, G. Evidence of an estrogen receptor form devoid of estrogen binding ability in MCF-7 cells. *Steroids* **2000**, *65*, 903−913.